FUSE

Fungal Systematics and Evolution

VOLUME 16
DECEMBER 2025
PAGES 41–53

doi.org/10.3114/fuse.2025.16.3

Exploring *Neopestalotiopsis* diversity associated with Blueberry leaf and twig blight in South African nurseries

L.S. Van der Vyver[1], W. De Bruin[1], N. Siyoum[1], D.L. Nsibo[1,3], J.Z. Groenewald[2], P.W. Crous[2,3], L. Korsten[1*]

[1]Department of Plant and Soil Sciences, University of Pretoria, Pretoria, South Africa
[2]Westerdijk Fungal Biodiversity Institute, Uppsalalaan 8 3584 CT, Utrecht, The Netherlands
[3]Forestry and Agricultural Biotechnology Institute (FABI), University of Pretoria, South Africa

*Corresponding author: lise.korsten@up.ac.za

Key words:
Neopestalotiopsis
nursery
phylogeny
South Africa
taxonomy
Vaccinium corymbosum

Abstract: New blueberry plantings in South Africa have increased dramatically since the year 2000, exceeding the global expansion rate. The crop is, however, impacted by several economically important fungal pathogens. Lesser-known fungi such as pestalotioid species can cause leaf and twig blight, and have the potential to become a global threat to blueberry production and expansion. This study aimed to assess the presence of such fungal species in blueberry nurseries in South Africa due to the industry's exponential growth and mass introduction of new cultivars. Symptomatic leaf and twig samples were collected from six propagation nurseries, resulting in 180 pestalotioid isolates, of which a subset of 48 isolates were selected for molecular characterisation using multi-locus sequence analysis of the internal transcribed spacer region (ITS), partial translation elongation factor 1-α (*TEF1*) and partial β-tubulin (*TUB2*) gene regions. Phylogenetic analyses were performed using Maximum Likelihood, Maximum Parsimony and Bayesian Inference methods. Based on the phylogenetic analyses, all isolates clustered with three previously described species of *Neopestalotiopsis*, namely *N. rosae*, *N. hispanica* and *N. longiappendiculata.* Of these, 32 isolates were identified as *N. rosae,* followed by *N. hispanica* (12) and *N. longiappendiculata* (4). To the best of our knowledge, this is the first report of these species in South Africa. Based on phylogenetic analysis and morphological comparisons, we further recommend that *N. vaccinii* be considered a synonym of *N. hispanica.*

Citation: Van der Vyver LS, De Bruin W, Siyoum N, Nsibo DL, Groenewald JZ, Crous PW, Korsten L (2025). Exploring *Neopestalotiopsis* diversity associated with Blueberry leaf and twig blight in South African nurseries. *Fungal Systematics and Evolution* **16**: 41–53. doi: 10.3114/fuse.2025.16.3
Received: 4 February 2025; **Accepted:** 5 March 2025; **Effectively published online:** 13 May 2025
Corresponding editor: A.J.L. Phillips

INTRODUCTION

Blueberries (*Vaccinium corymbosum*) belong to the family *Ericaceae* and are perennial shrubs that bear tasty and highly nutritious fruits (Milivojevic *et al.* 2012). These nutrient-dense fruits are rich in vitamins, fibre and antioxidants such as flavonoids and phenolic acids (Krishna *et al.* 2023). Due to their nutritional value, global demand has increased, leading to a 5.12 % rise (from 1,769530 to 1,860080 tons) between 2021 and 2022. America was the leading producer during this time, contributing 920080 tons. In South Africa, blueberry production grew by 17.31 % (from 26000 to 30500 tons) between 2022 and 2023, with most growth in the Western Cape Province (Pienaar *et al.* 2019, IBO 2023).

Blueberry cultivation in South Africa is primarily divided between shade netting and open-field production, with 17 % of blueberries grown under plastic covers (Pienaar *et al.* 2019). The two main varieties grown are the southern highbush (SHB) and the northern highbush (NHB). Due to limited chilling hours, SHB is predominantly grown in the southern coastal regions, whereas NHB is grown in the central areas of South Africa (Retamales & Hancock 2018). To ensure the healthy growth and expansion of the industry, it is therefore essential to assess which potential fungal pathogens occur in nursery material. This knowledge is critical for the development and implementation of effective disease-management strategies.

Leaf and twig blight symptoms have been observed in some newly planted blueberry fields and other production regions and nurseries in South Africa. These types of symptoms are generally caused by *Botrytis cinerea*, *Alternaria alternata* and *Botryosphaeria dothidea* (Milholland 1972, Wright *et al.* 2004, Rivera *et al.* 2013). Other fungi that can affect blueberry plants pre- and post- harvest are *Colletotrichum gloeosporioides*, *Diaporthe vaccinii* and *Pucciniastrum minimum*, leading to fruit decay, twig blight and leaf rust (Hartung 1981, Cardinaals *et al.* 2018, Anderson 2022). While most of these pathogens are economically important, there is also a need to characterise lesser-known pathogens, such as pestalotioid fungi, which can be overlooked when investigating causal agents of leaf and twig blight. These fungal species are known to be plant pathogens and can pose a major concern in a rapidly expanding industry. Some of these species can under conditions of high humidity, long periods of leaf wetness and wounding cause symptoms similar to other well-known blueberry leaf diseases (Belisário *et al.* 2020).

Pestalotioid fungi have also been reported to cause blueberry canker and twig dieback (Borrero *et al.* 2018), strawberry fruit rot (Baggio *et al.* 2021), tea leaf blight (Shahriar *et al.* 2021) and blueberry leaf spot (Zheng *et al.* 2023) in Spain, Florida, Malaysia and China, respectively. *Pestalotiopsis* was first described by Steyaert (1949) and later revised by Guba (1961). However, a molecular-based phylogenetic evaluation of these species was conducted by Hu *et al.* (2007). While the diversity of *Pestalotiopsis* was assessed using culture morphology and molecular methods using the ITS region, species identification became possible only after incorporating sequence data from the partial β-tubulin gene region (*TUB2*) into phylogenetic analyses (Hu *et al.* 2007). Subsequently, Maharachchikumbura *et al.* (2012) evaluated 10 genes and identified ITS, partial translation elongation factor 1-α (*TEF1*) and *TUB2* as suitable for identifying *Pestalotiopsis* species. This led to their further classification in 2014, dividing *Pestalotiopsis* into three genera: *Pestalotiopsis*, *Neopestalotiopsis* and *Pseudopestalotiopsis*, distinguished through phylogenetic analyses and colouration of conidial median cells (Maharachchikumbura *et al.* 2014). The aforementioned genera include endophytes (Gideon *et al.* 2018), saprophytes (Liu *et al.* 2008) and phytopathogenic species (Crous *et al.* 2011). To date, only *N. natalensis* has been documented in South Africa on *Acacia mollissima* (black wattle) (Maharachchikumbura *et al.* 2014). Phytopathogenic pestalotioid species such as *Pestalotiopsis neglecta* (Espinoza *et al.* 2008), *N. clavispora* (Borrero *et al.* 2018, Lee *et al.* 2019, Jevremović *et al.* 2022), *N. rosae* (Rodríguez-Gálvez *et al.* 2020) and *N. vaccinii* (Santos *et al.* 2021) have been reported on blueberries from Chile, Spain, Korea, Serbia, Peru and Portugal, respectively. The presence of pestalotioid fungi in blueberry nurseries of South Africa is currently unknown, an aspect which this study aimed to address.

MATERIALS AND METHODS

Sample collection and fungal isolation

In 2023, symptomatic blueberry leaves and twigs were collected from six propagation nurseries across the northern and southern production regions of South Africa. One nursery was located in Gauteng Province, while the remaining five were situated in Western Cape Province. Leaves and twigs were removed with pruning shears that had been surface-sterilised with 70 % ethanol. Samples were individually stored in paper bags and transported in a cooler box to the Plant Pathology laboratories of the University of Pretoria and stored overnight at 4 °C for immediate processing. Fungal isolation was performed according to the method described by Liu *et al.* (2015). Leaf and twig samples were surface sterilised with 70 % ethanol and 1 % sodium hypochlorite for 1 min each and then rinsed three times in sterile distilled water. Samples were dried on sterile paper towels in laminar flow cabinets. Leaf tissue from the margin of the diseased areas was aseptically removed (5 mm^2), placed onto half-strength potato dextrose agar (PDA) and incubated at 25 °C in the dark. After five d, 180 *Neopestalotiopsis* fungal colonies were sub-cultured from the margin of the colony onto full-strength PDA and incubated at 25 °C in the dark. To obtain pure cultures, representative isolates were purified by hyphal tipping onto full-strength PDA plates and incubated at 25 °C in the dark. Based on their cultural morphology, 48 of the 180 isolates were selected as group representatives for identification.

Culture preparation and morphological analysis

The cultural characteristics and conidiomata of the 48 isolates were observed in cultures grown on PDA at 25 °C in darkness for five days, then at 20 °C under a 12 h light/dark cycle for an additional 7 d. Digital images of all structures were recorded with an Axiocam 105 colour camera mounted on a Zeiss Axioskop 2 plus compound microscope with differential interference contrast illumination. Conidiomatal morphology was examined using a Keyence VHX-7000 digital dissecting microscope. Microscope preparations were mounted in a 20 % glycerol solution. A Nikon Eclipse E200 compound microscope was used to make 30 measurements of each structure. Conidial length was measured from the base of the apical appendages to the base of the basal cell and conidial width was measured across the widest conidial segment. The length and width values were reported as one standard deviation (SD) above and below the mean, with extreme measurements shown in parentheses, followed by the mean ± SD. All other measurements were provided as the full range, from the lowest to the highest extremes. Colony colours were determined using a mycological colour chart (Rayner 1970). Cultures with an (ex-)type status are indicated with a superscript T throughout the text.

DNA extraction, PCR amplification and sequencing

Genomic DNA was extracted from 7–14-d-old cultures using a Quick-DNA Fungal/Bacterial Miniprep Kit (Zymo Research, USA) following the manufacturer's instructions. Extracted DNA was stored at -20 °C until further use. The internal transcribed spacer (ITS) regions and intervening 5.8S nrRNA gene of the nrDNA was amplified with the primers ITS1 (5'-TCCGTAGGTGAACCTGCGG-3') and ITS4 (5'-TCCTCCGCTTATTGATATGC-3') (White *et al.* 1990). The partial β-tubulin (*TUB2*) gene was amplified with the primers Bt2a (5'-GGTAACCAAATCGGTGCTGCTTTC-3') and Bt2b (5'-ACCCTCAGTGTAGTGACCCTTGGC-3') (Glass & Donaldson 1995). The partial translation elongation factor 1-α (*TEF1*) gene was amplified with the primers EF1-728F (5'- CATCGAGAAGTTCGAGAAGG-3') and EF1-986R (5'-TACTTGAAGGAACCCTTACC-3') (Carbone & Kohn 1999). The PCR mixture consisted of 12.5 µL DreamTaq Green PCR Master Mix (2×) (Thermo Scientific, Germany), 0.25 µL (2 µm) of each forward and reverse primer, 11 µL of PCR grade ddH2O and 1 µL of template DNA. Thermocycling conditions for the amplification of ITS and *TUB2* were as follows: initial denaturation at 95 °C for 2 min; followed by 35 cycles of 94 °C for 30 s, 57 °C for 45 s and 72 °C for 90 s; and a final extension at 72 °C for 7 min. Part of the *TEF1* gene was amplified as described by Udayanga *et al.* (2012). Initial denaturation was performed at 95 °C for 5 min, followed by 40 cycles at 95 °C for 30 s, 58 °C for 50 s and 72 °C for 60 s and a final elongation at 72 °C for 10 min. Thermocycling was performed using Mastercycler Pro Thermocycler S (Eppendorf, Germany).

The amplified PCR products were purified using a Smarted Nucleic Acid Kit (Stratec, Germany), according to the manufacturer's guidelines. The purified amplicon was further amplified with a BigDye Terminator v. 3.1 Cycle Sequencing Kit (Thermo Scientific, Germany). The PCR mixture consisted of 0.5 µL of BigDye Terminator v. 3.1 Ready Reaction Mix, 1 µL (2 µm) forward or reverse primers, 2.5 µL of 5× sequencing Buffer, 4 µL of ddH2O and 2 µL of purified amplicon DNA to serve as a template. Terminator thermocycling conditions for all amplicons were as follows: initial denaturation at 96 °C for 1 min, followed by 25 cycles at 96 °C for 10 s, 50 °C for 5 s and 60 °C for 4 min. The resulting product was precipitated with ethanol before submission to the University of Pretoria's Sanger Sequencing facility at the Faculty of Natural and Agriculture sciences using an ABI3500xL Genetic analyser Applied Biosystems, ThermoFisher Scientific, USA).

Phylogenetic analyses

The DNA sequences of ITS, *TUB2* and *TEF1* were used for phylogenetic analyses. Additional sequences that served as reference data were obtained from GenBank (www.ncbi.nlm.nih.gov/genbank/) and are listed in Table 1. A total of 118 strains were selected for phylogenetic analysis, of which 48 were isolated in this study and 70 served as reference strains, including one outgroup taxon. Sequences were aligned with MAFFT v. 7 (https://mafft.cbrc.jp/alignment/server/index.html). The resulting alignment was manual improvement using Mesquite v. 3.81. (Maddison & Maddison 2023) and MEGA v. 11.0.13 (Tamura *et al.* 2021). Multi-locus phylogenetic analysis was performed using Maximum Likelihood (ML), Maximum Parsimony (MP) and Bayesian inference (BI). Inference of the ML partitioned alignment was achieved using RAxML v. 8.2.10 (Stamatakis 2014). One thousand rapid bootstraps were used to determine the support values for the optimal ML tree. The "-m GTRGAMMA" parameter was used in the RAxML analysis to estimate and optimise unique alpha-shaped parameters, GTR rates and empirical base frequencies for each partition. A final optimised likelihood score was used by the software to select the final tree among suboptimal trees. The MP was performed using PAUP (Phylogenetic Analysis Using Parsimony) v. 4.0a. build 169 (Swofford 2003). Trees were inferred using the heuristic search option with 1000 random sequence additions and TBR branch swapping. A total of 1000 bootstrap replications were used to evaluate the robustness of the equally most parsimonious trees. Optimal nucleotide substitution models were determined prior to the Bayesian analysis using MrModeltest v. 2.4 (Nylander 2004) in conjunction with PAUP. The BI analyses were done with MrBayes v. 3.3.7a (Rodríguez-Gálvez *et al.* 2020). Four Markov Chain Monte Carlo chains ran simultaneously over a maximum of 1000 M generations, terminating when the standard deviation of split frequencies reached 0.01 with a burn-in factor of 0.25. Trees were sampled every 10 generations and the trees were summarised and posterior probability values were calculated from the trees remaining after removal of the burn-in trees. The alignment and phylogenetic trees were deposited at www.figshare.com (doi: 10.6084/m9.figshare.28302329).

Congruence between single locus and concatenated trees were assessed based on overall topography by visualisation in FigTree v. 1.4.4 (http://tree.bio.ed.ac.uk/software/figtree/) and modified in the Inkscape Project (https://inkscape.org).

RESULTS

Phylogenetic analyses

The resulting concatenation of the three-locus alignment contained a total of 1288 nucleotide positions, including gaps (ITS: 549, *TEF1*: 318, and *TUB2*: 421). The best ML tree was obtained with an optimised likelihood of -4390,954206 (Fig. 1). The MP analysis determined 881 characters to be constant, 281 to be variable characters and 126 to be parsimony-informative characters. The heuristic analysis revealed 1000 equally most parsimonious trees with 749 steps (CI = 0.656, RI = 0.762, RC = 0.499, HI = 0.344). MrModelTest selected the following best-fit models for the different partitions for the Bayesian analysis: for ITS, the HKY+I model includes a proportion of invariable sites; for *TEF1*, the HKY+G model applies a gamma distribution for rate variation; and for *TUB2*, the GTR+G model uses gamma-distributed rates. Dirichlet (1,1,1,1) state frequency distribution was determined to be suitable for the MrBayes analyses across all partitions. The BI analysis ran until the standard deviation of split frequencies reached 0.01 after 62,600000 generations. A total of 12,520002 trees were saved, 75 % of which were used to calculate the 50 % majority rule consensus tree and the posterior probabilities. The ML, MP and BI phylogenetic trees showed similar species-level topologies.

Of the 48 isolates used in the present study, 32 isolates formed a poorly supported cluster with *N. rosae* (CBS 101057^{T}), with ML bootstrapping (MLB), MP bootstrapping (MPB) and BI posterior probability (PP) support values of 59/-/0.52. The Pairwise comparison (blast2) between the novel sequences in the clade and the ex-type sequences of *N. rosae* (CBS 101057^{T}) were highly similar across all gene regions. On ITS: 99 % (over 476/492 nt including one gap), *TEF1*: 100 % (over 244/276 nt) and *TUB2*: 100 % (over 405/405 nt).

An additional 12 isolates clustered with *N. hispanica* (CBS 147686^{T}) and *N. vaccinii* (CAA1059^{T}) with moderate support values of 86/87/0.77 (MLB/MPB/PP). The microscopic morphologies of *N. hispanica* (CBS 147686^{T}) and *N. vaccinii* (CAA1059^{T}) were compared together with an isolate from our study that clustered in the same clade (Table 2), as described by Diogo *et al.* (2021) and Santos *et al.* (2021). One of our isolates, BBFC0176, resembled *N. hispanica* in all parameters. However, when comparing *N. hispanica* to *N. vaccinii*, the length of the conidia, basal appendage, apical appendage and number of apical appendages did not correlate. When considering the concatenated alignment, the *TEF* and *TUB2* gene regions were identical with the only differences between *N. hispanica* (CBS 147686^{T}) and *N. vaccinii* (CAA1059^{T}) being a single nucleotide deletion in the ITS region. Pairwise comparisons (blast2) between the novel sequences generated in this study to the ex-type sequences of *N. hispanica* (CBS 147686^{T}) revealed a high degree of similarity across all gene regions. On ITS: 99 % (over 474/475 nt including one gap and 473/476 including two gaps), *TEF1*: 100 % (over 251/259 nt) and *TUB2*: 100 % (over 354/397 nt).

The remaining four isolates clustered with *N.*

Fig. 1. Maximum-likelihood phylogram tree generated by RAxML-based analysis of the concatenated (ITS+*TEF1+TUB2*) alignment. Maximum-likelihood bootstrapping (MLB), maximum-parsimony bootstrapping (MPB) above 50 % and Bayesian inference posterior probabilities (PP) above 0.5 (MLB/MPB/PP) are shown. Isolates from the current study isolated from blueberry are printed in red with identified/synonymised taxa in respective superscripts. Reference (ex-)type strains indicated by superscript T. The tree is rooted to *Pestalotiopsis diversiseta* (MFLUCC 12-0297^{T}).

Table 1. GenBank accession numbers of isolates used in this study for the phylogenetic analyses of *Neopestalotiopsis* species.

Species	Strain[1]	GenBank Accession number		
		ITS	***TEF1***	***TUB2***
Neopestalotiopsis acrostichi	MFLUCC 17-1754 [T]	MK764272	MK764316	MK764338
N. alpapicalis	MFLUCC 17-2544 [T]	MK357772	MK463547	MK463545
N. aotearoa	CBS 367.54 [T]	KM199369	KM199526	KM199454
N. asiatica	MFLUCC 12-0286 [T]	JX398983	JX399049	JX399018
N. australis	CBS 114159 [T]	KM199348	KM199537	KM199432
N. brachiate	MFLUCC 17-1555 [T]	MK764274	MK764318	MK764340
N. brasiliensis	COAD 2166 [T]	MG686469	MG692402	MG692400
N. camelliae-oleiferae	CSUFTCC81 [T]	OK493585	OK507955	OK562360
N. cavernicola	KUMCC 20-0269 [T]	MW545802	MW550735	MW557596
N. chrysea	MFLUCC 12-0261 [T]	JX398985	JX399051	JX399020
N. clavispora	MFLUCC 12-0281 [T]	JX398979	JX399045	JX399014
N. coffea-arabicae	HGUP4015 [T]	KF412647	KF412644	KF412641
N. cubana	CBS 600.96 [T]	KM199347	KM199521	KM199438
N. dendrobii	MFLUCC 14-0106 [T]	MK993571	MK975829	MK975835
N. drenthii	BRIP 72263a [T]	MZ303786	MZ344171	MZ312679
N. egyptiaca	CBS 140162 [T]	KP943747	KP943748	KP943746
N. eucalypticola	CBS 264.37 [T]	KM199376	KM199551	KM199431
N. eucalyptorum	CBS 147684 [T]	MW794108	MW805397	MW802841
N. foedans	CGMCC 3.9123 [T]	JX398987	JX399053	JX399022
N. formicarum	CBS 362.72[T]	KM199358	KM199517	KM199455
N. fragariae	ZHKUCC 22-0115	ON651146	ON685197	ON685199
N. guajavae	FMB0026 [T]	MF783085	MH460868	MH460871
N. guajavicola	FMB0129 [T]	MH209245	MH460870	MH460873
N. hadrolaeliae	VIC 47180 [T]	MK454709	MK465122	MK465120
N. haikouensis	SAUCC212271 [T]	OK087294	OK104877	OK104870
N. hispanica	CBS 147686 [T]	MW794107	MW805399	MW802840
	BBFC0104	**PV018578**	**PV033977**	**PV033929**
	BBFC0151	**PV018579**	**PV033978**	**PV033930**
	BBFC0152	**PV018580**	**PV033979**	**PV033931**
	BBFC0176	**PV018581**	**PV033980**	**PV033932**
	BBFC0222	**PV018582**	**PV033981**	**PV033933**
	BBFC0229	**PV018583**	**PV033982**	**PV033934**
	BBFC0235	**PV018584**	**PV033983**	**PV033935**
	BBFC0241	**PV018585**	**PV033984**	**PV033936**
	BBFC0243	**PV018586**	**PV033985**	**PV033937**
	BBFC0250	**PV018587**	**PV033986**	**PV033938**
	BBFC0265	**PV018588**	**PV033987**	**PV033939**
	BBFC0273	**PV018589**	**PV033988**	**PV033940**
N. honoluluana	CBS 114495 [T]	NR_145245	KM199548	KM199457
N. hydeana	MFLUCC 20-0132 [T]	MW266069	MW251129	MW251119
N. hypericin	KUNCC 22-12597 [T]	OP498010	OP713768	OP765908
N. iberica	CBS 147688 [T]	MW794111	MW805402	MW802844
N. javaensis	CBS 257.31 [T]	KM199357	KM199543	KM199437
N. longiappendiculata	CBS 147690[T]	MW794112	MW805404	MW802845
	BBFC0259	**PV018590**	**PV033989**	**PV033941**
	BBFC0266	**PV018591**	**PV033990**	**PV033942**
	BBFC0268	**PV018592**	**PV033991**	**PV033943**

Table 1. (Continued).

Species	Strain[1]	GenBank Accession number		
		ITS	***TEF1***	***TUB2***
	BBFC0300	**PV018593**	**PV033992**	**PV033944**
N. lusitanica	MEAN 1317 [T]	MW794110	MW805406	MW802843
N. maddoxii	BRIP 72266a [T]	MZ303782	MZ344167	MZ312675
N. mesopotamica	CBS 336.86 [T]	KM199362	KM199555	KM199441
N. mianyangensis	CGMCC 3.23554[T]	OP546681	OP723490	OP672161
N. musae	MFLUCC 15-0776 [T]	NR_156311	KX789685	KX789686
N. nebuloides	BRIP 66617 [T]	MK966338	MK977633	MK977632
N. olumideae	BRIP 72273a [T]	MZ303790	MZ344175	MZ312683
N. paeoniae-suffruticosae	CGMCC 3.23555[T]	OP082292	OP204794	OP235980
N. perukae	FMB0127 [T]	MH209077	MH523647	MH460876
N. petila	MFLUCC 17-1738 [T]	MK764275	MK764319	MK764341
N. phangngaensis	MFLUCC 18-0119 [T]	MH388354	MH388390	MH412721
N. photiniae	MFLUCC 22-0129 [T]	OP498008	OP753368	OP752131
N. protearum	CBS 114178 [T]	JN712498	KM199542	KM199463
N. psidii	FMB0028 [T]	MF783082	MH460874	MH477870
N. rhizophorae	MFLUCC 17-1550 [T]	MK764277	MK764321	MK764343
N. rhododendi	MFLUCC 22-0130[T]	OP497995	OP753370	OP762671
N. rhododendri	GUCC 21504[T]	MW979577	MW980444	MW980443
N. rhododendricola	KUN-HKAS-123204 [T]	OK283069	OK274148	OK274147
N. rosae	CBS 101057 [T]	KM199359	KM199523	KM199429
	BBFC0122	**PV018594**	**PV033993**	**PV033945**
	BBFC0131	**PV018595**	**PV033994**	**PV033946**
	BBFC0135	**PV018596**	**PV033995**	**PV033947**
	BBFC0175	**PV018597**	**PV033996**	**PV033948**
	BBFC0177	**PV018598**	**PV033997**	**PV033949**
	BBFC0178	**PV018599**	**PV033998**	**PV033950**
	BBFC0179	**PV018600**	**PV033999**	**PV033951**
	BBFC0180	**PV018601**	**PV034000**	**PV033952**
	BBFC0181	**PV018602**	**PV034001**	**PV033953**
	BBFC0186	**PV018603**	**PV034002**	**PV033954**
	BBFC0187	**PV018604**	**PV034003**	**PV033955**
	BBFC0188	**PV018605**	**PV034004**	**PV033956**
	BBFC0189	**PV018606**	**PV034005**	**PV033957**
	BBFC0199	**PV018607**	**PV034006**	**PV033958**
	BBFC0201	**PV018608**	**PV034007**	**PV033959**
	BBFC0202	**PV018609**	**PV034008**	**PV033960**
	BBFC0205	**PV018610**	**PV034009**	**PV033961**
	BBFC0206	**PV018611**	**PV034010**	**PV033962**
	BBFC0207	**PV018612**	**PV034011**	**PV033963**
	BBFC0208	**PV018613**	**PV034012**	**PV033964**
	BBFC0209	**PV018614**	**PV034013**	**PV033965**
	BBFC0217	**PV018615**	**PV034014**	**PV033966**
	BBFC0223	**PV018616**	**PV034015**	**PV033967**
	BBFC0245	**PV018617**	**PV034016**	**PV033968**
	BBFC0249	**PV018618**	**PV034017**	**PV033969**
	BBFC0251	**PV018619**	**PV034018**	**PV033970**
	BBFC0255	**PV018620**	**PV034019**	**PV033971**

Table 1. (Continued).

Species	Strain[1]	GenBank Accession number		
		ITS	*TEF1*	*TUB2*
	BBFC0256	**PV018621**	**PV034020**	**PV033972**
	BBFC0261	**PV018622**	**PV034021**	**PV033973**
	BBFC0262	**PV018623**	**PV034022**	**PV033974**
	BBFC0267	**PV018624**	**PV034023**	**PV033975**
	BBFC0298	**PV018625**	**PV034024**	**PV033976**
N. rosicola	CFCC 51992 ^{T}	KY885239	KY885243	KY885245
N. samarangensis	MFLUCC 12-0233 ^{T}	JQ968609	JQ968611	JQ968610
N. saprophytica	MFLUCC 12-0282 ^{T}	KM199345	KM199538	KM199433
N. sichuanensis	SM15-1C^{T}	MW166232	MW199751	MW218525
N. siciliana	CBS 149117 ^{T}	ON117813	ON107273	ON209162
N. sonneratae	MFLUCC 17-1745 ^{T}	MK764279	MK764323	MK764345
N. subepidermalis	CFCC 55160 ^{T}	OK560699	OM622425	OM117690
N. suphanburiensis	MFLUCC 22-0126- ^{T}	OP497994	OP753372	OP752135
N. surinamensis	CBS 450.74 ^{T}	KM199351	KM199518	KM199465
N. terricola	CGMCC 3.23553^{T}	OP082294	OP204796	OP235982
N. thailandica	MFLUCC 17-1730 ^{T}	MK764281	MK764325	MK764347
N. umbrinospora	MFLUCC 12-0285 ^{T}	JX398984	JX399050	JX399019
N. vaccinii	CAA1059 ^{T}	MW969747	MW959099	MW934610
N. vacciniicola	CAA1055 ^{T}	MW969749	MW959101	MW934612
N. vheenae	BRIP 72293a ^{T}	MZ303792	MZ344177	MZ312685
N. vitis	MFLUCC 15-1265 ^{T}	KU140694	KU140676	KU140685
N. zakeelii	BRIP 72282a ^{T}	MZ303789	MZ344174	MZ312682
N. zimbabwana	CBS 111495 ^{T}	JX556231	KM199545	KM199456
Outgroup: *Pestalotiopsis diversiseta*	MFLUCC 12–0287 ^{T}	JX399009	JX399073	JX399040

[1]CBS: Culture Collection of the Westerdijk Fungal Biodiversity Institute, Utrecht, The Netherlands; CGMCC: China General Microbial Culture Collection Center (China); MFLUCC: Mae Fah Luang University Culture Collection, Chiang Rai, Thailand; BRIP: Queensland Plant Pathology Herbarium, Brisbane, Queensland, Australia; FMB: Department of Plant Pathology, University of Agriculture Faiasalabad, Jail Road, Faisalabad, Punjab, Pakistan; CAA: Personal Culture Collection Artur Alves, Department of Biology, University of Aveiro; ZHKUCC: Uppsala University Culture Collection, Sweden.
Isolates and sequences from the current study printed in bold.
Reference (ex)-type strains indicated by supescript T.

Table 2. Microscopic morphological comparison of *N. hispanica* (CBS 147686^{T}), *N. vaccinii* (CAA1059^{T}) and isolate BBFC0176.

Morphology (µm)	*N. vaccinii* (CAA1059^{T})	*N. hispanica* (CBS 147686^{T})	Isolate BBFC0176
Conidiogenous cells length	(1.3–)14.1–19.9(–25.8)	7–14.7	7-20.5
Conidiogenous cells width	(2.1–)2.7–3.0(–3.7)	2.4–4.1	3.2-5.9
Conidia length	(11.0–)13.4–13.8(–15.2)	(21.5–)24.4–25.3(–27.1)	(20.1–) 20.8-26.7 – (27.9)
Conidia width	(4.9–)6.3–6.6(–7.5)	(5.9–)7.2–7.8(–8.7)	(6.1–) 6.2-7.9 (–8.3)
Basal cell	(2.2–)2.9–3.6(–6.3)	3.3–5.5	3.5–6.6
Apical cell	(2.4–)3.7–4.3(–5.1)	2.8–6.2	2.5-4.7
Basal appendage	1.7–6.6	5.1–15.5	2-9.8
Apical appendage	8.9–25.3	(30.7–)19.5–22.6(–30.7)	(16.9–) 17-27.4 (–41.4)
Appendage number	2–3	3–4	3–4

longiappendiculata (MEAN 1315[T]) with high support values, 89/90/1 (MLB/MPB/PP). Pairwise comparison (blast2) between novel sequences generated in this study to the ex-type sequence of *N. longiappendiculata* (MEAN 1315[T]) revealed high similarity across all gene regions. On ITS: 100 % (over 481/492 nt), *TEF1*: 100 % (over 259/259 nt) and *TUB2*: 99 % (over 404/405 nt).

Taxonomy

Neopestalotiopsis hispanica E. Diogo *et al.*, *Mycol. Progr.* **20**: 1448. 2021. Fig. 2.
Synonym: *Neopestalotiopsis vaccinii* J. Santos *et al.*, *Eur. J. Pl. Path.* **162**: 549. 2021.

Pycnidial conidiomata (BBFC0176) on PDA, globose, semi-immersed, black, 183–527 µm; exuding globose, black, glistening conidial masses. *Conidiophores* indistinct, often reduced to conidiogenous cells. *Conidiogenous cells* discrete, cylindrical, hyaline, smooth-walled, simple, proliferating percurrently, tapering towards a truncated apex, 5.9–19.0 × 2.4–7.0 µm. *Conidia* fusoid, ellipsoid, straight or slightly curved with 4 septa (21.2–)21.7–27.2(–28.6) × (5.6–)5.7–7.9(–7.9) µm, $\bar{x}$ ± SD = 24.3 ± 1.8 × 6.6 ± 0.6 µm; basal cell; conic with truncated base, hyaline, rugose and thin-walled, 2.9–6.3 µm, with a single, tubular, unbranched, centric basal appendage 1.6–8 µm long; three median cells doliiform 15–17.7 µm long, $\bar{x}$ ± SD = 16.2 ± 0.8 µm, wall rugose, versicoloured, with septa darker than the rest of the cell; second cell from base pale brown, 3.4–6 µm long; third cell honey brown, 4.4–6.6 µm long; fourth cell brown, 4.4–6.4 µm long; apical cell 3.3–5.6 µm long, hyaline cylindrical, thin with smooth walls; 3–4 apical appendages, inserted each in upper half of apical cell, unbranched, filiform, (19.5–)20.8–38.6(–39.1) long, $\bar{x}$ ± SD = 30.8 ± 7.2 µm.

Culture characteristics: On PDA cultures reached 56 mm diam. after 7 d at 25 °C with irregular margins, pale-yellow,

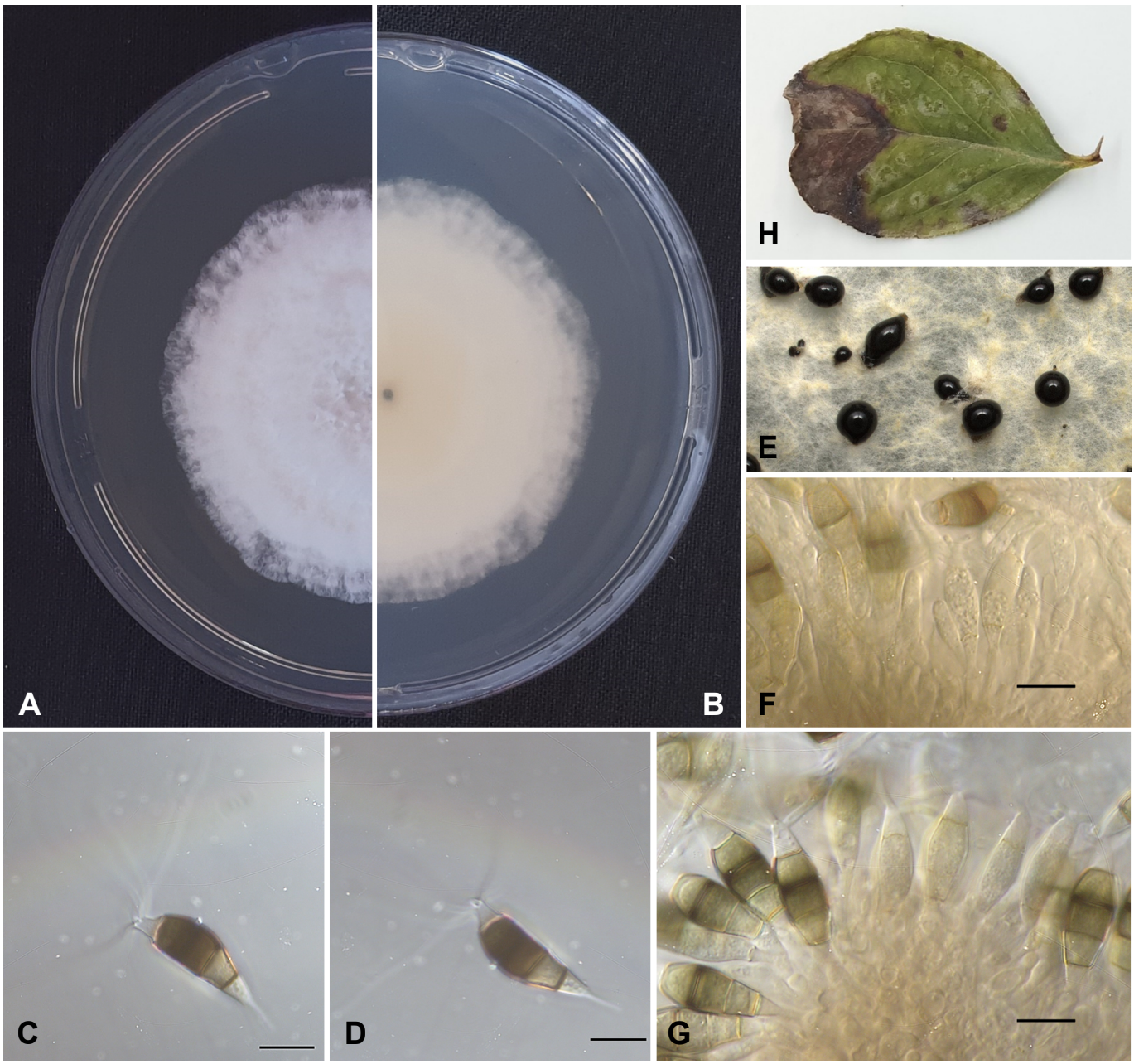

Fig. 2. Morphology of *Neopestalotiopsis hispanica* (BBFC0176) isolated from *Vaccinium corymbosum*. **A.** Upper culture surface. **B.** Reverse culture surface on PDA after 7 d at 25 °C. **C, D.** Conidia. **E.** Conidiomata on PDA. **F, G.** Conidiogenous cells. **H.** Sampled leaf. Scale bars = 10 µm.

with aerial mycelium conidiomata prevalent on mycelium margins (Fig. 2).

Neopestalotiopsis longiappendiculata E. Diogo *et al*., *Mycol. Progr*. **20**: 1450. 2021. Fig. 3.

Pycnidial conidiomata (BBFC0266) on PDA, globose, semi-immersed, black, 272−357 µm; exuding globose, black, glistening conidial masses. *Conidiophores* indistinct, often reduced to conidiogenous cells. *Conidiogenous cells* discrete, cylindrical, hyaline, smooth-walled, simple, proliferating percurrently, tapering towards a truncated apex, 10.6−17.5 × 3.1−7.8 µm. *Conidia* fusoid, ellipsoid, straight or slightly curved with four septa (17.3−)17.5−25.9(−26.5) × (5.9−)6.1−7.8(−8.0) µm, $\bar{x}$ ± SD = 21.1 ± 2.2 × 7 ± 0.5 µm; basal cell; conic with truncated base, hyaline, rugose and thin-walled, 2.1−5.3 µm, with a single, tubular, unbranched, centric basal appendage 1.7−11.4 µm long; three median cells doliiform (11.7–)12–17.3(–17.8) µm long, $\bar{x}$ ± SD = 14.2 ± 1.5 µm, wall rugose, versicoloured, with septa darker than the rest of the cell; second cell from base pale brown, 2.8–6.2 µm long; third cell honey brown, 3.6–5.9 µm long; fourth cell brown, 4.1–6.1 µm long; apical cell 2.9–5.2 µm long, hyaline cylindrical, thin with smooth walls; 3–4 apical appendages, inserted each in upper half of apical cell, unbranched, filiform, (12.2−)12.7−23.9(−24.3) long, $\bar{x}$ ± SD = 19.1 ± 3.2 µm.

Culture characteristics: On PDA cultures reached 32 mm diam. after 7 d at 25 °C with irregular margins, pale yellow, with aerial mycelium conidiomata prevalent on mycelium margins (Fig. 3).

Neopestalotiopsis rosae Maharachch. *et al.*, *Stud. Mycol*. **79**: 147. 2014. Fig. 4.

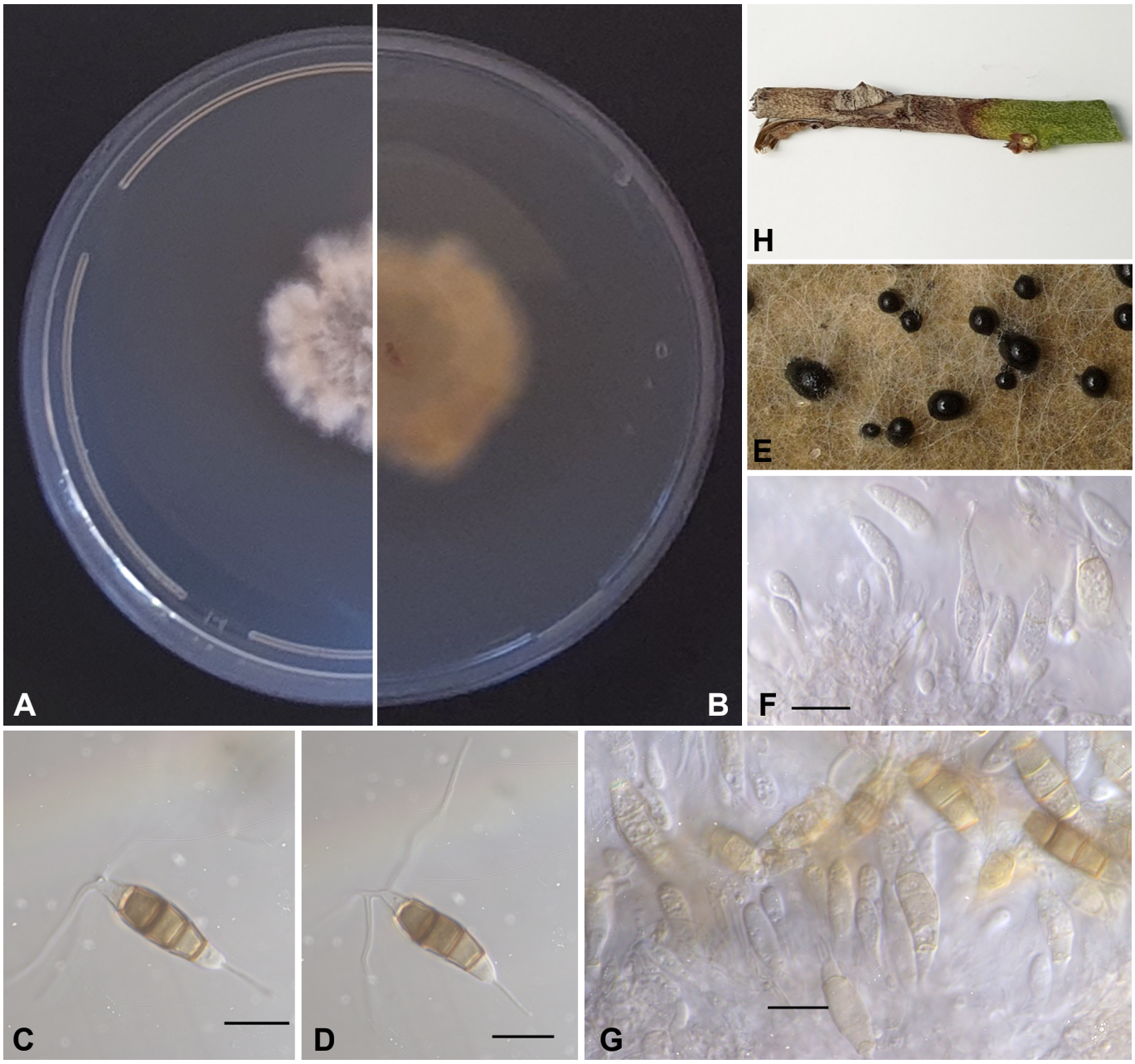

Fig. 3. Morphology of *Neopestalotiopsis longiappendiculata* (BBFC0266) isolated from *Vaccinium corymbosum*. **A.** Upper culture surface. **B.** Reverse culture surface on PDA after 7 d at 25 °C. **C, D.** Conidia. **E.** Conidiomata on PDA. **F, G.** Conidiogenous cells. **H.** Sampled twig. Scale bars = 10 µm.

Pycnidial conidiomata (BBFC0178) on PDA, globose, semi-immersed, black, 236–527 µm; exuding globose, black, glistening conidial masses. *Conidiophores* indistinct, often reduced to conidiogenous cells. *Conidiogenous cells* discrete, cylindrical, hyaline, smooth-walled, simple, proliferating percurrently, tapering towards a truncated apex, 7.0–20.5 × 3.2–5.9 µm. *Conidia* fusoid, ellipsoid, straight or slightly curved with 4 septa (20.1–)20.8–26.7(–27.9) × (6.1–)6.2–7.9(–8.3) µm, $\bar{x}$ ± SD = 23.5 ± 1.9 × 6.9 ± 0.6 µm; basal cell; conic with truncated base, hyaline, rugose and thin-walled, 2.8–5.3 µm, with a single, tubular, unbranched, centric basal appendage 2.0–9.8 µm long; three median cells doliiform (13.2–)13.9–16.9(–16.9) µm long, $\bar{x}$ ± SD = 15.5 ± 0.9 µm, wall rugose, versicoloured, with septa darker than the rest of the cell; second cell from base pale brown, 3.5–6.6 µm long; third cell honey brown, 4.2–6.6 µm long; fourth cell brown, 3.9–6.1 µm long; apical cell 2.5–4.7 µm long, hyaline cylindrical, thin with smooth walls; 3–5 apical appendages, inserted each in upper half of apical cell, unbranched, filiform, (16.9–)17.0–27.4(–41.4) long, $\bar{x}$ ± SD = 23.3 ± 3 µm.

Culture characteristics: On PDA cultures reached 59 mm diam. after 7 d at 25 °C with irregular margins, pale-yellow, with aerial mycelium conidiomata prevalent on clearly visible concentric mycelium (Fig. 4).

DISCUSSION

In this study, 48 *Neopestalotiopsis* isolates from six nurseries in South Africa were identified through molecular characterisation using multi-locus phylogenetic analyses of ITS, *TEF1* and *TUB2* genes. The resulting ML, MP and BI phylogenetic trees showed similar species-level topology when compared to previous studies (Maharachchikumbura

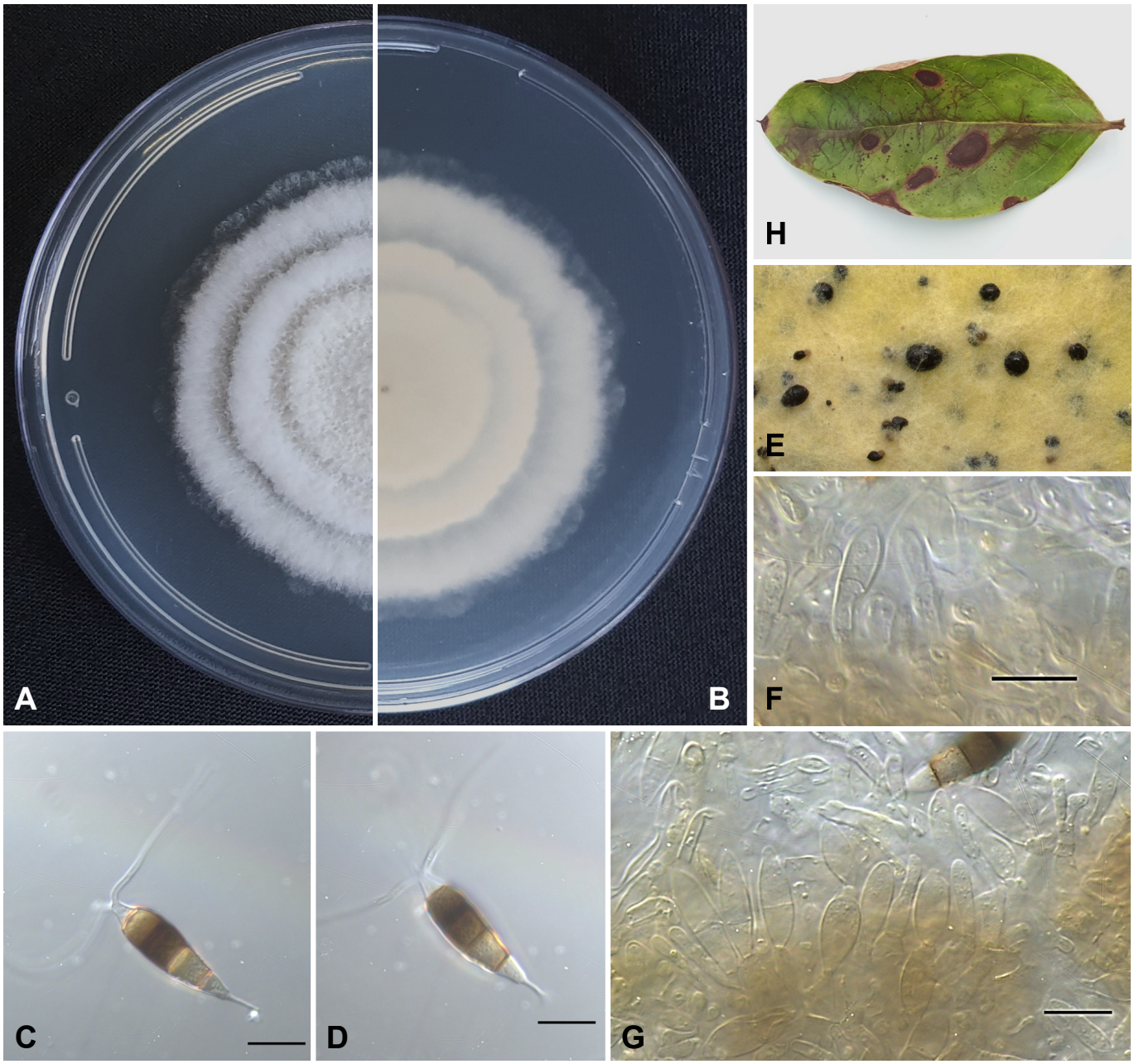

Fig. 4. Morphology of *Neopestalotiopsis rosae* (BBFC0178) isolated from *Vaccinium corymbosum*. **A.** Upper culture surface. **B.** Reverse culture surface on PDA after 7 d at 25 °C. **C, D.** Conidia. **E.** Conidiomata on PDA. **F, G.** Conidiogenous cells. **H.** Sampled leaf. Scale bars = 10 µm.

et al. 2014, Solarte *et al.* 2018, Darapanit *et al.* 2021, Santos *et al.* 2021). *Neopestalotiopsis rosae* was the most abundant (59 %), followed by *N. hispanica* (29 %) and *N. longiappendiculata* (12 %). A related study conducted in Portugal investigated twig-associated pestalotioid fungi in blueberry orchards and identified species of *Pestalotiopsis* and *Neopestalotiopsis* (Santos *et al.* 2021). No species of *Pestalotiopsis* were found in the current study from blighted twigs or leaves, only species of *Neopestalotiopsis.*

Since its initial description by Guba (1961), *N. rosae* has emerged globally as a significant plant pathogen that causes various diseases in a range of plant species. It has been identified as the causal agent of blueberry dieback and stem blight in Peru (Rodríguez-Gálvez *et al.* 2020), strawberry root rot, fruit rot and leaf spot in Mexico (Rebollar-Alviter *et al.* 2020), pomegranate leaf and fruit spot in Florida (Xavier *et al.* 2020), avocado dieback and stem blight in Italy (Fiorenza *et al.* 2022) and leaf and fruit spot of pecan in China (Gao *et al.* 2022). During 2019–2020, strawberry production in Florida (USA) suffered losses due to *N. rosae*, causing leaf and fruit spots and ultimately reducing the vigour of the affected plants. The outbreak affected 18 commercial farms, leading to the estimated destruction of 80 ha of strawberry production fields to prevent the spread to unaffected areas. A strawberry nursery selling infected plant material was suggested as the source of the outbreak (Baggio *et al.* 2021).

Neopestalotiopsis rosae was identified as a pathogen on the blueberry varieties 'Biloxi' and 'Duke' in studies by (Rodríguez-Gálvez *et al.* 2020, Santos *et al.* 2021). Pathogenicity trials conducted on the 'Duke' variety showed that both *N. rosae* and *N. vaccinii* produced significant lesions on the stems, with *N. rosae* resulting in considerably larger lesions compared to *N. vaccinii*. Additionally, *N. rosae* further retarded the growth of inoculated blueberry plants more than any other tested species of *Neopestalotiopsis* (Santos *et al.* 2021). Based on its history in strawberry nursery settings and blueberry orchards, *N. rosae* can become a serious threat to blueberry nursery and orchard production in South Africa.

Neopestalotiopsis rosae differs from *N. javaensis* by having longer conidial appendages and at the molecular level by 2 nt in ITS and 5 nt in *TEF1.* These characteristics are often used to confirm identity as these species are very closely related (Maharachchikumbura *et al.* 2014, Diogo *et al.* 2021). In our study, the BI phylogeny was unable to differentiate between these species. However, the maximum likelihood phylogenetic tree generated by RAxML successfully did so, supported by apical appendage measurements. This is possibly due to the limited nucleotide substitution models available when using RAxML. This highlights the importance of utilising ML, MP and BI instead of relying on only one or the other. Furthermore, the primer sets used for the amplification of the three gene regions in the current study only partially overlap (ITS: 95.4 %; *TEF1*: 55.9 %; *TUB2*: 55.2 %) with the study done by (Maharachchikumbura *et al.* 2014).

A total of 12 isolates from our study formed a well-supported clade with *N. vaccinii* (CAA1059^{T}) and *N. hispanica* (CBS 147686^{T}). *Neopestalotiopsis vaccinii* has only been reported in association with blueberries, isolated from twig dieback, twig blight and necrotic leaf symptoms in blueberry orchards of Portugal (Santos *et al.* 2021). *Neopestalotiopsis hispanica*, on the other hand, has only been described on *Eucalyptus globulus*, which was found in stem girdling and dieback tissue from a nursery in Portugal (Diogo *et al.* 2021). Due to the absence of sufficient taxonomical and molecular features to confidently distinguish *N. vaccinii* and *N. hispanica*, we regard them as synonymous. The name *N. hispanica* should be used, as it was published first (8 Nov. 2021 versus 22 Nov. 2021) in accordance with the International Code of Nomenclature for algae, fungi and plants (Turland *et al.* 2018), and therefore has priority.

Lastly, four isolates from our study formed a well-supported clade with *N. longiappendiculata* (CBS 147690^{T}), which was also first isolated from *Eucalyptus globulus* tissue in the aforementioned study in Portugal (Diogo *et al.* 2021). Furthermore, *N. longiappendiculata* was also found to cause grey blight on leaves of *Camellia* spp. in China (Wang *et al.* 2022). Our finding expands the host range of *N. longiappendiculata*, marking its first documented occurrence on blueberry.

This study is the first to record the presence of *N. rosae* and *N. hispanica* in symptomatic blueberry leaves and twigs in South African nurseries, while *N. longiappendiculata* was identified exclusively on symptomatic twigs. We recommend that future studies investigate the pathogenicity of all three species of *Neopestalotiopsis* on blueberry varieties to determine if they warrant a more effective prevention of introduction and control strategy as part of a plant improvement programme.

ACKNOWLEDGEMENTS

The authors are grateful to the nurseries for their willingness to participate in this study investigating present species of *Neopestalotiopsis* in South Africa. This research was supported by the South African berry industry, Berries ZA.

Conflict of interest: The authors declare that they have no conflict of interest.

REFERENCES

Anderson J (2022). *Pucciniastrum minimum* (blueberry leaf rust). In: CABI Compendium Wallingford, UK: CAB International. https://doi.org/10.1079/cabicompendium.11863

Baggio JS, Forcelini BB, Wang N-Y*, et al.* (2021). Outbreak of leaf spot and fruit rot in Florida strawberry caused by *Neopestalotiopsis* spp. *Plant Disease* **105**: 305–315. https://doi.org/10.1094/PDIS-06-20-1290-RE

Belisário R, Aucique-Pérez CE, Abreu LM*, et al.* (2020). Infection by *Neopestalotiopsis* spp. occurs on unwounded eucalyptus leaves and is favoured by long periods of leaf wetness. *Plant Pathology* **69**: 194–204. https://doi.org/10.1111/ppa.13132

Borrero C, Castaño R, Avilés M (2018). First report of *Pestalotiopsis clavispora* (*Neopestalotiopsis clavispora*) causing canker and twig dieback on blueberry bushes in Spain. *Plant Disease* **102**: 1178. https://doi.org/10.1094/PDIS-10-17-1529-PDN

Carbone I, Kohn LM (1999). A method for designing primer sets for speciation studies in filamentous ascomycetes. *Mycologia* **91**: 553–556. https://doi.org/10.1111/ppa.13132

Cardinaals J, Wenneker M, Voogd JGB*, et al.* (2018). Pathogenicity

of *Diaporthe* spp. on two blueberry cultivars (*Vaccinium corymbosum*). *EPPO Bulletin* **48**: 128–134. https://doi.org/10.1111/epp.12451

Crous PW, Summerell BA, Swart L, *et al.* (2011). Fungal pathogens of *Proteaceae*. *Persoonia* **27**: 20–45. https://doi.org/10.3767/003158511X606239

Darapanit A, Boonyuen N, Leesutthiphonchai W, *et al.* (2021). Identification, pathogenicity and effects of plant extracts on *Neopestalotiopsis* and *Pseudopestalotiopsis* causing fruit diseases. *Scientific Reports* **11**: 1–11. http://doi.org/10.1038/s41598-021-02113-5

Diogo E, Gonçalves CI, Silva AC, *et al.* (2021). Five new species of *Neopestalotiopsis* associated with diseased *Eucalyptus* spp. in Portugal. *Mycological Progress* **20**: 1441–1456. http://doi.org/10.1007/s11557-021-01741-5

Espinoza JG, Briceño EX, Keith LM, *et al.* (2008). Canker and twig dieback of blueberry caused by *Pestalotiopsis* spp. and a *Truncatella* sp. in Chile. *Plant Disease* **92**: 1407–1414. http://doi.org/10.1094/PDIS-92-10-1407

Fiorenza A, Gusella G, Aiello D, *et al.* (2022). *Neopestalotiopsis siciliana sp. nov*. and *N. rosae* causing stem lesion and dieback on avocado plants in Italy. *Journal of Fungi* **8**: 562. http://doi.org/10.3390/jof8060562

Gao Y, Zhai FY, Zhang YB, *et al.* (2022). *Neopestalotiopsis rosae* causing black spot on leaf and fruit of *Pecan* (*Carya illinoinensis*) in China. *Plant Disease* **106**: 1995. http://doi.org/10.1094/PDIS-07-21-1541-PDN

Gideon OA, Jones OM, Bakare AG, *et al.* (2018). Metabolites from endophytic fungus; *Pestalotiopsis clavispora* isolated from *Phoenix reclinata* leaf. *Future Journal of Pharmaceutical Sciences* **4**: 273–275. https://doi.org/10.1016/j.fjps.2018.10.001

Glass NL, Donaldson GC (1995). Development of primer sets designed for use with the PCR to amplify conserved genes from filamentous ascomycetes. *Applied and Environmental Microbiology* **61**: 1323–1330. http://doi.org/10.1128/aem.61.4.1323-1330.1995

Guba EF (1961). *Monograph of Monochaetia and Pestalotia*. Harvard University Press, Cambridge, Mass.

Hartung JS (1981). Epidemiological studies of blueberry anthracnose disease caused by *Colletotrichum gloeosporioides*. *Phytopathology* **71**: 449. https://doi.org/10.1094/Phyto-71-449

Hu H, Jeewon R, Zhou D, *et al.* (2007). Phylogenetic diversity of endophytic *Pestalotiopsis* species in *Pinus armandii* and *Ribes* spp.: evidence from rDNA and β-tubulin gene phylogenies. *Fungal Diversity* **24**: 1–22.

IBO (2023). International Blueberry Organisation. *Global State of the Blueberry Industry Report*. California, United States of America. https://www.internationalblueberry.org/2023-report

Jevremović D, Vasić T, Živković S, *et al.* (2022). *Neopestalotiopsis clavispora:* a causal agent of twig dieback on highbush blueberries in Serbia. *Journal of Plant Diseases and Protection* **129**: 1277–1283. http://doi.org./10.1007/s41348-022-00610-x

Krishna P, Pandey G, Thomas R, *et al.* (2023). Improving blueberry fruit nutritional quality through physiological and genetic interventions: A review of current research and future directions. *Antioxidants* **12**: 810. https://doi.org/10.3390/antiox12040810

Lee Y, Kim GH, Kim Y, *et al.* (2019). First report of twig dieback caused by *Neopestalotiopsis clavispora* on blueberry in Korea. *Plant Disease* **103**: 1022. http://doi.org/10.1094/PDIS-10-18-1734-PDN

Liu F, Weir BS, Damm U, *et al.* (2015). Unravelling *Colletotrichum* species associated with *Camellia*: employing ApMat and GS loci to resolve species in the *C. gloeosporioides* complex. *Persoonia* **35**: 63–86. http://doi.org/10.3767/003158515X687597

Liu L, Liu S, Jiang L, *et al.* (2008). Chloropupukeananin, the first chlorinated pupukeanane derivative, and its precursors from *Pestalotiopsis fici*. *Organic Letters* **10**: 1397–1400. http://doi.org/10.1021/ol800136t

Maddison WP, Maddison DR (2023). *Mesquite: a modular system for evolutionary analysis*. Version 3.81. http://www.mesquiteproject.org.

Maharachchikumbura SSN, Guo L-D, Cai L, *et al.* (2012) A multi-locus backbone tree for *Pestalotiopsis*, with a polyphasic characterization of 14 new species. *Fungal Diversity* **56**: 95–129. https://doi.org/10.1007/s13225-012-0198-1

Maharachchikumbura SSN, Hyde KD, Groenewald JZ, *et al.* (2014). *Pestalotiopsis* revisited. *Studies in Mycology* **79**: 121–186. http://doi.org/10.1016/j.simyco.2014.09.005

Milholland R (1972). Histopathology and pathogenicity of *Botryosphaeria dothidea* on blueberry stems. *Phytopathology* **62**: 654–660. http://doi.org/10.1094/Phyto-62-654

Milivojevic J, Maksimovic V, Maksimovic JD, *et al.* (2012). A comparison of major taste-and health-related compounds of *Vaccinium* berries. *Turkish Journal of Biology* **36**: 738–745. http://doi.org/10.3906/biy-1206-39

Nylander JAA (2004). *MrModeltest V2.* Program distributed by the author. Evolutionary Biology Centre, Uppsala University.

Pienaar L, Mzwanele L, Philips S (2019). *The economic contribution of the South African blueberry industry.* https://www.berriesza.co.za/wp-content/uploads/2021/01/BlueberryIndustryReport_2019FINAL.pdf.

Rayner RW (1970). *A mycological colour chart*. Commonwealth Mycological Institute; British Mycological Society, Kew, England.

Rebollar-Alviter A, Silva-Rojas HV, Fuentes-Aragón D, *et al.* (2020). An emerging strawberry fungal disease associated with root rot, crown rot and leaf spot caused by *Neopestalotiopsis rosae* in Mexico. *Plant Disease* **104**: 2054–2059. http://doi.org/10.1094/PDIS-11-19-2493-SC

Retamales JB, Hancock JF (2018). Blueberries. 2nd edn. In: *Crop production science in horticulture*. CABI, Wallingford, United Kingdom. https://doi.org/10.1079/9781780647265.0000

Rivera SA, Zoffoli JP, Latorre BA (2013). Infection risk and critical period for the postharvest control of gray mold (*Botrytis cinerea*) on blueberry in Chile. *Plant Disease* **97**: 1069–1074. https://doi.org/10.1094/PDIS-12-12-1112-RE

Rodríguez-Gálvez E, Hilário S, Lopes A, *et al.* (2020). Diversity and pathogenicity of *Lasiodiplodia* and *Neopestalotiopsis* species associated with stem blight and dieback of blueberry plants in Peru. *European Journal of Plant Pathology* **157**: 89–102. http://doi.org/10.1007/s10658-020-01983-1

Santos J, Hilário S, Pinto G, *et al.* (2021). Diversity and pathogenicity of pestalotioid fungi associated with blueberry plants in Portugal, with description of three novel species of *Neopestalotiopsis*. *European Journal of Plant Pathology* **162**: 539–555. http://doi.org/10.1007/s10658-021-02419-0

Shahriar SA, Nur-Shakirah AO, Mohd MH (2021). *Neopestalotiopsis clavispora* and *Pseudopestalotiopsis camelliae-sinensis* causing grey blight disease of tea (*Camellia sinensis*) in Malaysia. *European Journal of Plant Pathology* **162**: 709–724. http://doi.org/10.1007/s10658-021-02433-2

Solarte F, Muñoz CG, Maharachchikumbura SSN, *et al.* (2018). Diversity of *Neopestalotiopsis* and *Pestalotiopsis* spp., causal agents of guava scab in Colombia. *Plant Disease* **102**: 49–59.

http://doi.org/10.1094/PDIS-01-17-0068-RE

Stamatakis A (2014). RAxML Version 8: a tool for phylogenetic analysis and post-analysis of large phylogenies. *Bioinformatics* **30**: 1312–1313. http://doi.org/10.1093/bioinformatics/btu033

Steyaert RL (1949). Contribution à l'étude monographique de *Pestalotia* de Not. et *Monochaetia* Sacc. (*Truncatella gen. nov*. et *Pestalotiopsis gen. nov*.). *Bulletin Jardin Botanic Éat Bruxelles* **39**: 285–354. https://doi.org/10.2307/3666710

Swofford D (2003). *PAUP*: Phylogenetic analysis using parsimony (* and other methods).* Version 4 Sinauer Associates, Sunderlands, Massachusetts.

Tamura K, Stecher G, Kumar S*, et al.* (2021). MEGA11: Molecular Evolutionary Genetics Analysis Version 11. *Molecular Biology and Evolution* **38**: 3022–3027. http://doi.org/10.1093/molbev/msab120

Turland NJ, Wiersema JH, Barrie FR*, et al.* (2018). *International Code of Nomenclature for algae, fungi, and plants (Shenzhen Code) adopted by the Nineteenth International Botanical Congress Shenzhen, China, July 2017. Regnum Vegetabile 159. Glashütten.*, Koeltz botanical books. https://doi.org/10.12705/Code.2018

Udayanga D, Liu X, Crous PW*, et al.* (2012). A multi-locus phylogenetic evaluation of *Diaporthe* (*Phomopsis*). *Fungal Diversity* **56**: 157–171. http://doi.org/10.1007/s13225-012-0190-9

Wang Q-T, Cheng Y-H, Zhuo L*, et al.* (2022). *Neopestalotiopsis longiappendiculata* as the agent of grey blight disease of *Camellia* spp. *Journal of Phytopathology* **170**: 770–777. http://doi.org/10.1111/jph.13139

White TJ, Bruns T, Lee S, *et al*. (1990). Amplification and direct sequencing of fungal ribosomal RNA genes for phylogenetics. In: *PCR protocols: a guide to methods and applications* (Innis MA, Gelfand DH, Sninsky JJ, *et al*., eds). *Academic Press, Inc*., New York, USA: 315–322. https://doi.org/10.1016/B978-0-12-372180-8.50042-1

Wright ER, Rivera MC, Esperón J*, et al.* (2004). Alternaria leaf spot, twig blight, and fruit rot of highbush blueberry in Argentina. *Plant Disease* **88**: 1383. https://doi.org/10.1094/PDIS.2004.88.12.1383B

Xavier K, Yu X, Vallad GE (2020). First report of *Neopestalotiopsis rosae* causing foliar and fruit spots on pomegranate in Florida. *Plant Disease* **105**: 504. http://doi.org/10.1094/PDIS-06-20-1282-PDN

Zheng X, Liu X, Li X*, et al.* (2023). *Pestalotiopsis* species associated with blueberry leaf spots and stem cankers in Sichuan Province of China. *Plant Disease* **107**: 149–156. https://doi.org/10.1094/PDIS-07-21-1550-RE